HHS Public Access

Author manuscript

J Phys Chem C Nanomater Interfaces. Author manuscript; available in PMC 2019 December 16.

Published in final edited form as:

J Phys Chem C Nanomater Interfaces. 2019 July 11; 123(27): 16495–16507. doi:10.1021/acs.jpcc.9b00913.

What Does Nanoparticle Stability Mean?

Hoa T. Phan, **Amanda J. Haes***

Department of Chemistry, University of Iowa, Iowa City, Iowa 52242, United States

Abstract

The term “nanoparticle stability” is widely used to describe the preservation of a particular nanostructure property ranging from aggregation, composition, crystallinity, shape, size, and surface chemistry. As a result, this catch-all term has various meanings, which depend on the specific nanoparticle property of interest and/or application. In this feature article, we provide an answer to the question, “What does nanoparticle stability mean?”. Broadly speaking, the definition of nanoparticle stability depends on the targeted size dependent property that is exploited and can only exist for a finite period of time given all nanostructures are inherently thermodynamically and energetically unfavorable relative to bulk states. To answer this question specifically, however, the relationship between nanoparticle stability and the physical/chemical properties of metal/metal oxide nanoparticles are discussed. Specific definitions are explored in terms of aggregation state, core composition, shape, size, and surface chemistry. Next, mechanisms of promoting nanoparticle stability are defined and related to these same nanoparticle properties. Metrics involving both kinetics and thermodynamics are considered. Methods that provide quantitative metrics for measuring and modeling nanoparticle stability in terms of core composition, shape, size, and surface chemistry are outlined. The stability of solution-phase nanoparticles are also impacted by aggregation state. Thus, collision and DLVO theories are discussed. Finally, challenges and opportunities in understanding what nanoparticle stability means are addressed to facilitate further studies with this important class of materials.

Graphical Abstract

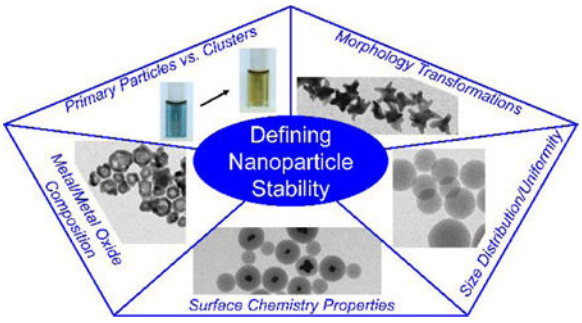

*Phone: (319) 384-3695. Fax (319) 335-1270. amanda-haes@uiowa.edu.

AUTHOR INFORMATION

The manuscript was written through contributions of all authors. All authors have given approval to the final version of the manuscript.

The authors declare no competing financial interest.

1. INTRODUCTION

Nanoparticles are defined as objects with at least one dimension that ranges from 1–100 nm[1] thereby influencing a size-dependent property.[2] As a material's dimension decreases from bulk to the nanoscale, both the surface area to volume ratio[3–4] and surface energy[5] increase. Because all nanoscale features exhibit higher energies compared to bulk materials, all nanoscale objects are in a non-thermodynamically favored state in comparison to bulk materials under standard room temperature and pressure conditions. As such, nanomaterial phases can be considered as metastable, that is, in a short-lived energetic state relative to macroscale materials. As a result, defining nanoparticle stability is ubiquitous in the discussion of all nanomaterials and their size dependent properties as evidenced by a growing number of previous studies on this topic.[6] Herein, we focus on metal and metal oxide nanoparticles as well as their stability-dependent properties ranging from catalytic,[7–8] optoelectrical,[9–11] magnetic,[12–14] mechanic,[15] and thermal.[16] The initial metastable state of these materials depends on the synthetic route used to generate the nanomaterials of interest.[6, 17–18] Because of the extensive literature on nanoparticle synthesis, we have focused this feature article on nanomaterial changes post-synthesis, that is, during storage and/or subsequent use.

Upon formation, nanoparticle stability is often defined in terms of the specific size dependent property that is exploited in a particular application. For instance, El-Sayed et. al.[19] evaluated how hydroxyl-terminated poly(amido-amine) (PAMAM) dendrimers, block copolymer polystyrene-b-poly(sodium acrylate), and poly(N-vinyl-2-pyrrolidone) (PVP) influenced Pd nanoparticle stability post-synthesis. In this case, nanoparticle stability was linked to the maintenance of metal surface area, which was subsequently related to the reduced probability of nanostructure aggregation. PAMAM dendrimer-stabilized Pd nanoparticles exhibited maximized catalytic activity followed by those stabilized by the block copolymer then PVP. This finding suggests that nanoparticle stability is related to the retention of a primary, non-aggregated particle state. Catalytic nanoparticle stability also depends on the conservation of active crystal facets[3, 7] on the nanoparticle surface and not just total nanoparticle surface area. For instance, Pt nanocubes (d=7 nm)[20] have been shown to more rapidly promote oxygen reduction than polyhedron (d=5 nm) or truncated cubes (d=3 nm). The greatest catalytic activity was observed for nanocubes while polyhedron and truncated cubes exhibited lower yet similar activities. Trends were not observed with respect to total surface area. Instead, catalytic activity depended on the amount of the highly active (100) crystal facet available. X-ray diffraction (XRD) patterns revealed that nanocubes, polyhedron, and truncated cubes possessed 91%, 24%, and 26% of (100) facets on their surfaces. Thus, the catalytic activities of these three nanostructures depend on the available surface area associated with Pt(100) facets as these promote oxygen reduction more readily than other crystal facets. Preferred crystal facets are dependent on the exact catalytic reaction targeted. Stability associated with catalytically-active Pt or Pd nanoparticles, therefore, depends on the retention and availability of relevant crystal facets. Common strategies that promote stability rely on the inclusion of stabilizing agents with direct dependencies on their size[19] and thickness[19] or indirect implications from variations in nanostructure surface potential.[17, 21] Both dependencies impact the likelihood of

nanostructure aggregation.[17, 22] It is important to note that surface chemistry, which promotes the presence of primary nanoparticles without preventing interactions between reactants and metal atoms, is needed for retention of catalytic activity.

In general, the three-dimensional morphology of nanostructures is directly correlated to total surface area availability, aggregation state, crystal facets, as well as the ability of nanoparticles to resist dissolution. This final consideration is of utmost importance when considering the activity associated with Ag nanoparticles.[23] In contrast to the examples associated with Pt and Pd nanoparticles, Ag nanoparticle stability was directly correlated with the lack of metal dissolution. In this case, surface sulfidation led to the formation of Ag_2S from Ag_2O ($K_{sp}=5.92 \times 10^{-51}$ vs. 4×10^{-11}, respectively). This chemical transformation reduced the likelihood of Ag^+ release into the natural environment and promoted primary nanoparticle suspension. In this example, stability is related to the retention of atomic concentration of the metal (silver) associated with the nanostructures. Common non-native surface chemistries include thin oxide,[24] sulfide,[23] or silica[25] layers, and the thickness and dielectric properties of these materials are tuned to promote a particular size-dependent property while suppressing dissolution or metal release into an environment.[19, 19, 21, 26, 17, 22, 23, 27]

In all of these studies, the term “nanoparticle stability” describes the preservation of nanostructure properties as a function of composition,[6] shape,[17] size,[28] and surface chemistry.[29] Size dependent properties and/or targeted applications have also been considered. Because of their remarkable size-dependent properties and vast applications, nanoparticle stability can mean very different things to scientists and engineers who make, model, and use these materials. The purpose of this feature article is to provide an overview of how to categorize and quantify nanoparticle stability so that we can better define what is meant when the term nanoparticle stability is used. To do this, metal/metal oxide nanoparticle stability is defined and categorized in terms of core composition, shape, size, and surface chemistry. An emphasis is also placed on nanoparticle aggregation of gas- and solution-phase nanostructures as this is an added concern for materials that can undergo collisions in a gaseous or liquid medium. Regardless of the definition for nanoparticle stability, methods that measure and allow for quantification of stability are described as this allows identification of specific metrics for monitoring potential transformations of these materials as a function of time. Finally, ongoing practical challenges and opportunities associated with the inherent metastability associated with metal and metal oxide nanoparticles are discussed. While infinite shelf-life cannot be expected for these materials, their many promising applications encourage further investigation.

2. DEFINITION AND MECHANISMS OF NANOPARTICLE STABILITY

Metal and metal oxide based materials are widely exploited in their macroscale form due to their catalytic, electric, optical, magnetic, mechanic, and thermal properties.[30] As their dimensions decrease to the nanoscale, the wavelength of light becomes large with respect to size,[2] the total surface area to volume ratio increases,[3–4] surface energy elevates,[5] and the number of low coordination surface atoms (relative to interior atoms) increases.[31] All of these size-dependent characteristics impact the electronic and crystal structure of these

materials and as a result, their chemical and physical properties as a function of composition,[12, 15] size,[4] and/or shape.[32–33] In order to maintain these properties for further application, understanding these transformations or by definition, stability, is relevant. As such and as summarized in Table 1, stability in terms of aggregation, metal/metal oxide composition, shape, size, and surface chemistry are discussed in this section.

Stability in Terms of Aggregation.

Aggregation,[17, 22] the most common indicator of gas- and solution-phase nanoparticle instability, occurs when primary nanostructures undergo clustering upon interactions at short distances.[65] As a result, nanoparticle stability depends on preventing these processes. Noble metal nanostructures[11] are excellent for visualizing aggregation as their plasmonic properties depend on interparticle distances and can be visually observed.[17] Dynamic light scattering (DLS)[66] is often used to monitor cluster formation for materials that are non-plasmonic. When all clusters overcome buoyancy forces, materials undergo sedimentation.[67]

For clusters to form, nanoparticles must physically collide thus collision theory is commonly used to model kinetics.[17, 22] The rate at which clusters form will depend on energetics (*vide infra*) and collision frequency (z). Assuming Brownian motion,[22] the probability that two objects collide depends on the root mean square velocity ($\langle \nu \rangle$-m/s) and number density of the nanoparticles. The root mean square velocity reduces to the following:[22]

$$\langle \nu \rangle = \left(\frac{8kT}{\pi \mu} \right)^{0.5} \quad \text{(Eq. 1)}$$

where k is the Boltzmann constant, T is temperature, and μ is the reduced mass of the objects. “Stable” nanostructures undergo elastic collisions and remain as primary nanoparticles after a collision. “Unstable” nanostructures, however, undergo inelastic interactions.[68] To predict if an elastic or inelastic collision will occur, a kinetic energy barrier (E_a) is estimated from calculating the probability (e^{-E_a/k_BT}) of collisional frequency and interaction pair potentials.[22]

Nanoparticle aggregation also depends on thermodynamics[65] or the total interaction pair potential that arises between two objects.[17, 22, 65] Derjaguin–Landau–Verwey–Overbeek_(DLVO) theory[17, 22, 67] facilitates the calculation of the total interaction potential between two objects as a function of separation distance (s) and radius of curvature (r). The attractive van der Waals interaction potential (Φ_A) becomes significant at short separation distances.[22] As size decreases to less than 100 nm, both the Hamaker constant and van der Waals interaction potential increase. Electrostatic interaction potentials (Φ_R), which give rise to repulsive forces between objects, depend on the Debye length (κ^{-1}). In the presence of surface chemistry, additional parameters help promote repulsive interactions between objects.[17, 22] These extended DLVO parameters include osmotic (V_{osm}) and elastic-steric (V_{ela}) interaction potentials, which arise from solvent induced pressure and molecular entropy variations in surface bound molecules (i.e., polymer, electrolyte coating, or natural organic matter), respectively.[22] At separation distances that are less than the ligand thickness, the ligands on adjacent object undergo elastic deformation and compression,

which leads to repulsive elastic-steric interaction potentials. Retention of this steric coating and relevant interaction potential is promoted through stabilizing intermolecular interactions (π-π interactions) and increasing the layer thickness. The sum of these interaction potentials allows for predictions of potential energies that arise between objects as a function of separation distance. Objects are likely to exhibit elastic conditions when the maximum potential energy (V_{max}) exceeds the kinetic energy barrier (E_a) calculated from collision theory.

When, however, collisions occur with more kinetic than potential energy, particle flocculation occurs, and the size dependent properties of primary nanostructures typically change. The probability that aggregation will occur decreases upon reducing collision frequency by decreasing storage time in a particular medium or particle concentration. This is not always feasible[9, 11] but parameters such as pH (using SiO_2, TiO_2, Al_2O_3, and ZnO)[67] and capping agents[17, 49, 51] (for metals) help increase the maximum potential energy barrier. This barrier is maximized for silica nanoparticles,[21, 69] for instance, where the electrostatic interaction potential increases at basic pH values. Citrate deprotonation on gold nanospheres[70] induces a similar effect. At short separation distance, self-assembled monolayer formation further promotes gold nanoparticle stabilization via increases in osmotic and elastic-steric [17]by increasing the molecular volume, weight, and/or packing density of the capping agents. Increasing alkyl chain length does not always prevent nanoparticle aggregation in organic solvents such as toluene, hexane, and carbon tetrachloride because osmotic interaction potential barriers are lowered in these solvents vs. polar solvents.[71] Ligands such as branched alkanoates and branched thiolates provide more entropic stability than alkyl chains in these same non-polar solvents.[71] As a consequence, the concentration of stably suspended nanoparticles attained in solution increased by 3–4 orders of magnitude when functionalized with ligands that promote higher entropic barriers versus what is achievable with alkyls. Mixed n-alkanoate monolayers composed of myristate (C_{14}) and docosanoate (C_{22}) increased the solubility of CdSe nanoparticles in organic solvents by ~10^6 compared to those functionalized with myristate only. The nanostructures stabilized by the mixed monolayer were deemed to exhibit anti-aggregation behavior, a result that was attributed to the interruption of crystalline packing of ligands on particle surfaces.

All in all, solution-phase nanoparticle stability relies on the energetics of collisions versus potential energy. Nanoparticle stability is promoted when the probability of elastic collisions increase. Using both collision theory and DLVO theory, relative estimations of these energies for solution-phase structures can be estimated so that “stability” is promoted. Preventing nanoparticle aggregation can only be achieved for finite times given the probability dependence. As such, awareness of factors that drive cluster formation can be considered so that realistic expectations in nanoparticle stability with respect to aggregation can be made.

Stability as a Function of Metal/Metal Oxide Composition.

Typically, the atomic composition of cores and surfaces of a nanostructure are chemically distinct because of differences in surface atom coordination,[5] so stability refers to the

retention of the original surface atom identity and coordination. [10]Because surface atoms on nanostructures have lower coordination numbers than bulk atoms, their reactivity is relatively higher. Instability then refers to either chemical composition variations or coordination number changes. Oxidation is a common example of a surface atom transformation or instability. Oxidation of silver nanoparticles,[72] for instance, leads to progressive dampening of plasmon resonance features. Silver oxide also undergoes dissolution to form Ag^+ in aqueous environments.[23] Both of these instabilities lead to changing reactivity and materials fate. [73–74,75–76,77]

Stability in terms of nanoparticle metal/metal oxide composition can be evaluated before, during, and/or after use so that changes in elemental or molecular structure can be monitored. Energy-dispersive X-ray spectroscopy (EDS) is a powerful technique for identifying primary as well as interfering chemical composition in these materials.[78–79] Upon high energy electron bombardment, a characteristic X-ray spectrum can be collected and subsequently used for both identification and mass quantification of elements present in a sample.[79] All elements except H and He can be detected.[80] Figure 1 demonstrates the successful analysis of iron oxide nanoparticles with EDS where clear evidence of Fe and O content was identified through X-ray spectra analysis.[76] XRD[73–74] is a parallel method that can link core composition to nanoparticle stability and has been shown to provide insight into how O and S[23, 74] contamination impacts nanoparticle morphology.[73] This was achieved by comparing XRD patterns before and after storage of ZnO supported Pd-Zn,[81] Ag,[23] Al,[82] Cu,[83] Zn,[84] and Ni[85] nanoparticles. In these cases, oxides influenced nanoparticle stability and/or morphology. In short, these techniques provide both qualitative and quantitative elemental analysis based on characteristic X-ray signals and structural parameters from metals, metal oxides, and interfering elements such as O or S. Parallel information regarding oxidation[86] and sulfidation[87] can be extracted from localized surface plasmon resonance (LSPR) spectra associated with plasmonic nanomaterials. Silver oxide conversion, for instance, caused the plasmon features to red shift and dampen[72] thus providing additional evidence of changes in the stability of nanoparticle cores.

Regardless of composition, nanoparticle stability in terms of metal/metal oxide composition depends on both kinetics and thermodynamics. Kinetic stability of the metal/metal oxide atoms is influenced by large elemental ionization energies[68] (minimum energy that ejects a ground state electron). For instance, it is well established that Ag is more easily oxidized than gold,[28, 46] a phenomenon attributed to their relative first ionization energies (7.58 eV (731 kJ/mol) and 9.23 eV (890 kJ/mol), respectively).[88] While the standard Gibbs free energy of formation (ΔG^0_{298}) for Au_2O_3 indicates a thermodynamically preferred state when temperature drops below 28 K,[89] Ag nanoparticles undergo transformation into silver oxide (Ag_2O) upon exposure to air regardless of the presence of stabilizing agents as shown in Figure 2. This is because Ag oxidation is thermodynamically favored under standard temperature and pressure conditions. The standard free energy of formation for this reaction is −11.25 kJ/mol.[6] As particle dimensionality decreases to the nanoscale, oxidation occurs more readily given the inverse relationship between ΔG^0_{298} and nanoparticle radius as follows:

$$\Delta G^{0}_{298}(r) = -11.25 - \frac{57.5}{r} \quad \text{(Eq. 2)}$$

Reduction potential depends on dimensionality as follows:[90]

$$\Delta E = E_{Nanoparticle} - E_{bulk} = \frac{-2\gamma V_m 1}{ZF \quad R} \quad \text{(Eq. 3)}$$

where $E_{nanoparticle}$ and E_{bulk} are the reduction potential of nanoparticles and bulk materials, respectively, γ is surface tension, V_m is the molar volume, and R is radius. Experimental results for silver[90] support this model in that a 0.1 V decrease in standard reduction potential of bulk silver occurs upon decreasing nanoparticle radius to 14 nm. Similar to oxidation, sulfidation occurs when H_2S is exposed to silver nanoparticles in the aqueous phase. In this example, the transformation of Ag nanoparticles into Ag_2S is more thermodynamically favored than Ag_2O because the solubility product constant (K_{sp}) of Ag_2S (5.92×10^{-51}) is smaller and thermodynamically preferred versus Ag_2O (4×10^{-11}).[88]

As shown above, chemical transformations such as oxidation and sulfidation reactions become more likely as material dimensionality decreases to the nanoscale[6, 23, 90] because the free energy of formation becomes more negative and the standard reduction potential decreases with decreasing nanoparticle size. As a result, nanoparticle metal/metal oxide composition exhibits worsening stability with decreasing size. As such, exposure to chemically reactive components should be limited as much as possible to promote stability. This can be accomplished using a thin exterior oxide layer of a more reactive metal versus the metal/metal oxide,[24] inert metal,[46, 50] graphene oxide,[91] or a complex surfactant.[92] All of these approaches have successfully been used to improve the stability of nanoparticle metal/metal oxide composition in response to reactive components in a medium. As an example, coating metallic nanoparticle such as Cu[24] with oxides of a relatively more reactive metal such as Al_2O_3, which has a more positive standard reduction potential than the original metal, are more chemically stable than uncoated Cu.

Alternatively, metal/metal oxide composition transformations can be halted through metal doping. Addition of dopant metals such as Ag or Au, which have relatively high redox potentials versus primary metals such as Cu,[93] successfully promotes electron transfer from the primary metal to the dopant. As such, the inherent structure of bi- and multi-metallic structures can improve these applications by preventing oxidation of the primary metal. These structures, however, can undergo transformations from solid to hollow structures,[94–95] an instability attributed to alloying/dealloying processes[96] and the Kirkendall effect.[97]

Alloying/dealloying processes are usually involved in nanoparticle syntheses that have multiple Galvanic replacement reactions. The alloying process results in the formation of homogeneous bi-metallic nanostructures. This thermodynamically stable state is preferred over pure metallic nanostructures. Dealloying processes are observed when there is an imbalance between dissolved metal atoms from and new metal atoms deposited on a nanostructure. This leads to the formation of lattice vacancies on the resulting objects. These processes, however, are not common post-synthesis if reactants are removed from the

solution. Another phenomenon that can affect nanoparticle morphology is the Kirkendall effect. This occurs most effectively at elevated temperatures (~373 K) [94] for bulk materials but is promoted at room temperatures at defect sites and in cavities on nanostructures.[95] Luckily, stability can be promoted by minimizing the Kirkendall effect by storing nanomaterials at ambient or low temperatures.

Although both metal/metal oxide isolation and doping approaches promote the compositional stability of nanoparticles, some challenges exist. For instance, nanoparticle encapsulation by another material improves the stability of the targeted nanomaterial, but this same layer prevents direct interactions between the original material and its environment. As a result, applications requiring direct contact between the original metal/metal oxide and its surroundings such as in catalytic and thermal-based applications can be limited. There are often added benefits for using this approach to stabilize plasmonic nanoparticles as a thin (2–5 nm) layer can both promote retention of the desired optical properties while also protecting the original metal/metal oxide from compositional transformations. In contrast, doping approaches overcome limitations of introducing a physical barrier; however, the number of carrier electrons in the particle is modified thus influencing the electrical properties of the material. As a result, both benefits and compromises to material properties need to be carefully considered when choosing methods aimed at improving stability in terms of the original nanoparticle metal/metal oxide composition.

Stability in Terms of Nanoparticle Shape.

Nanoparticle stability in terms of shape is defined as the conservation of the original local structure and radius of curvature at the atomic and nanoscales as these dimensions directly impact surface free energy.[5] This important stability descriptor leads to the retention of catalytic, plasmonic, and mechanical properties of nanostructures. Morphological changes lead to variations in surface facet percentages; therefore, instability in this context arises when surface energy decreases from shape variations. The catalytic activity of Pt nanostructures represents an excellent platform for this stability indicator.[20] Nanocubes with (100) surface facets exhibited deteriorating catalytic activity as atomic reorganization led to the formation of nanospheres with lower energy and less reactive (111) surface facets. Another example of surface atom instability was noted during the use of gold nanostars as surface-enhanced Raman scattering (SERS) substrates.[98] Atoms at the tips of the branched structures underwent structural rearrangement because of their relatively high surface energy. This caused the branches to shorten and plasmonic resonance wavelengths to blue-shift by ~200 nm, an effect that caused worsening SERS activity. Both of these examples emphasize the importance of defining stability in terms of nanoparticle shape as these directly influence the physicochemical properties of nanomaterials. Stability in terms of nanoparticle morphology can be assessed from changes in atomic crystal lattice and surface facets. These are most often monitored using X-ray diffraction[99] or high-resolution transmission electron microscopy (HR-TEM).[44, 100] Local structure changes are best assessed using TEM, atomic force microscopy (AFM),[47] and/or scanning electron microscopy (SEM).[101] HR-TEM has been shown to identify shape and surface-induced reconstructions of nanoparticle morphology.[102–103] For instance, surface defects on as-

synthesized gold nanorods[100] revealed that surface reconstruction led to the transformations of the (110) into (111) crystal facets. Similar examples for cerium oxide[104] and Pt nanoparticles[102] were also observed. All of these methods can reveal changes in nanometer length scale as long as spatial resolution is adequate. One method that is not limited to spatial resolution is LSPR spectroscopy, where variations in nanoparticle shape are also evident for plasmonic nanostructures. This is because of the dependence of the LSPR on the shape factor, χ, as described by Mie theory.[33] Any change in the length or width of Au nanorods, for instance, would result in variations in either the longitudinal or transverse spectral features.[105]

Changes in fine structural detail are important in terms of stability because the percentage of surface atoms to total atoms increases as the size of a solid object decreases. Surface atoms are inherently more unstable than interior atoms because they coordinate to relatively fewer adjacent atoms. As a result, surface atoms exert a radially inward force so that the distance between the surface and interior atoms are minimized, which can induce morphology changes.[5] For instance,[31] the (111) lattice constants for 3.3 and 1.3 nm CdS nanocrystals were determined to be 5.80 and 5.72 Å, respectively. This difference was used to explain the size-dependent surface tension of the studied nanocrystals to be ~2.5 N/m, a value ~3 times larger than bulk (0.75 N/m). Surface tension (γ) in units of N/m can be calculated for a particular facet plane as follows:[5]

$$\gamma = \frac{1}{2} N_b \varepsilon \rho_a \quad \text{(Eq. 4)}$$

where N_b is the number of coordinating atoms at that facet, ε is bond strength (J/mol), and ρ_a is surface atomic density. This means that surface tension is greatest for (110) facets vs. (100) and (111) planes because there are 5, 4, and 3 adjacent atoms per surface atom.[5] If given enough time, all materials proceed to a state where Gibbs free energy is minimized. As such, nanoparticle shape tends to undergo transformation to minimize overall surface energy (or surface tension) so that thermodynamically stable structures are attained.

There are two common mechanisms for practically reducing the surface energy of a nanostructure while retaining shape and include surface adsorption (chemical[44, 48, 106] and physical[107]) and surface area reduction.[5] Nanoparticle shape is preserved at the nanoscale when adsorption takes place because surface atoms are energetically stabilized. As such, atomic coordination of interior atoms remains the same thus reducing the probability of nanoparticle shape transformations. Complex nanostructures such as nanorods,[48, 100] nanostars,[44] and nanocubes[99] are more impacted by shape transformation in comparison to simpler structures. This is because the density of high energy facets (i.e., (100) and (110)) with low coordination surface atoms increases with added morphology complexity.[5] This can be observed in Figure 3 where (110) and (111) facets are observed along nanorod sides and ends, respectively.[48, 100] CTAB binds preferentially to the (110) surfaces thus promoting nanoparticle stability.

In the case of ultrathin gold nanowires (d ≅ 1.6 nm),[108] surfactants such as oleylamine selectively stabilize Au (001) facets allowing nanostructure growth at (111) planes. Similarly, highly uniform silver clusters with the formula Ag_{44}(p-MBA) $^{4-}$ and diameters of

~1.2 nm form in the presence of p-mercaptobenzoic acid. The formation of these structures depend on intermolecular interactions between both the ligands and metal atoms present.[109] As such, these examples indicate the power of molecular adsorption in forming and retaining nanostructure shape and uniformity.

In the absence of surface chemistry that decreases the energy of low coordination surface atoms, morphology transformations are common.[5] For example, desorption of capping agents from a nanostructure surface often induces shape transformations.[110–111] Surface ligand disruption can also lead to oxidative etching.[112] This process often occurs during reductive reactions that take place during or post synthesis. These processes can lead to instabilities (i.e., blunting) of sharp features such as at the corners and branch tips of nanocubes and nanostars, respectively. Oxygen promotes the activity of common etchants such as Cl^-. Fe^{3+}, CN^-, thereby leading to metal atom removal at high chemical potential features and shape transformations.[112] This effect promoted the formation of crystalline nanoparticles through the dissolution of multiply-twinned nanostructures that exhibited relatively higher reactivity.[113] If chloride and oxygen were included at early stages of the synthesis, multiply-twinned silver nanoparticles dissolved at a similar rate as silver ion reduction. These processes occurred until a single-crystalline nanoparticle phase formed. This example illustrates that the formation of nanostructures with crystal facets with low reactivity can improve the morphological uniformity of nanostructures.

In order to promote morphological stability during storage and experiments, effects of digestive ripening, another mechanism of shape instability, can be suppressed by adding ligands that adsorb to specific crystal facets or through O_2 and common etchant removal.[112] Common capping ligands that help prevent oxidative etching include CTAB,[48, 100] HEPES,[114] PVP,[115] and PEG.[116] In general, anionic, cationic, zwitterionic, and non-ionic molecules adsorb to nanostructure surfaces and when added in excess, can help resist shape transformations by reversibly binding to high energy facets on non-spherical nanostructures. A good example of this involves the retention of branches in the HEPES-containing parent solution after the synthesis of gold nanostars.[114] Similarly, PVP binds preferentially to the (100) facets on Ag nanocube faces thus promoting their shape stability post-synthesis.[115]

Another approach involves the functionalization of nanoparticles using molecules with strong binding energies to the metal/metal oxide surface atoms (i.e., sulfur to Au)[17] thus minimizing molecular desorption and shape restructuring. In all of these examples, retention of standard temperature and pressure conditions is important. The major drawback to functionalization is that morphological changes can occur if the exchangeable ligands in solution are not uniformly suspended.[117–118] These changes arise through digestive ripening processes and are promoted at elevated temperatures. To minimize these effects, ligand exchange should be carried out through the slow addition of the second, exchangeable ligand at room temperature to minimize effects of digestive ripening and nanoparticle aggregation.[17, 49] In all cases, surface ligand packing density, chemical composition, and potential all influence surface energy. As such, these studies emphasize the importance of surface energy in promoting nanostructure stability as a function of local crystal structure and radius of curvature.

Stability in Terms of Nanoparticle Size.

Stability in terms of nanoparticle size is defined as the preservation of nanoparticle dimensionality during storage and/or an experiment. Because the physicochemical properties of nanoscale metal/metal oxides are size dependent, instability refers to an increase or decrease in nanoparticle dimensionality that causes a significant variation in catalytic, optical, magnetic, mechanical, and thermal properties of materials. Magnetic nanoparticles,[12] for example, can exhibit superparamagnetism where the average magnetic moment of small particles is zero in the absence of an external magnetic field but increases rapidly upon application of an external field. This property is only observed for feature sizes that support single-domain behavior. Likewise, nanoparticles can become efficient thermal conductors with decreasing size. This is because diffusion coefficients are indirectly proportional to size; therefore, heat transfer is facilitated as nanoparticle diffusion coefficients increase and as size decreases. Thus, retention of nanostructure dimensions is required for reproducible chemical and physical properties of nanoscale metals and metal oxides. Nanoparticle dimensions can be imaged directly or inferred through movement in a solution. TEM and scanning electron spectroscopy (SEM) routinely provide spatial resolution down to 0.2–0.5 nm[119] and 0.4–1.6 nm,[120] respectively. Imaging materials using these techniques typically require that a sample is deposited and dried on a support thus only provide accurate nanoparticle dimensions if the material is not influenced by solvation and/or mobile surface chemistries/ions. Chemical transformation is common when the medium changes (i.e., oxidation). High-resolution images can also be measured using AFM[34, 121] as vertical and lateral resolutions of 0.1 and 0.2 nm,[122] respectively, can be achieved. As with any scanning probe microscopy, sampling is limited by scan rate, sample size, and probe properties. Other techniques including small-angle X-ray scattering technique (SAXS)[123] and DLS[121] can also be used to analyze nanostructure size in solution. Both SAXS and DLS rely on the Stokes-Einstein equation[124] to quantify nanoparticle size. DLS, for instance, facilitates the estimation of hydrated particle dimensions from translational diffusion coefficient (D) estimations from light scattering measurements.

Nanoparticle dimensions can be quantified directly from images[5, 122] or indirectly[121] from mobility and spectroscopy measurements. The complex dimensionality of core-nanostructures composed of Ag, Au, and SiO_2 is shown in Figure 4A.[46] Dimensions of the various components are clearly observed due to differences in how electrons interact with the various materials. Additional information can be assessed using SAXS as size, shape, and surface details can be determined.[123] The nucleation and growth of gold nanoparticles, for instance, was evaluated using SAXS. Details related to size[125] and shape (i.e., nanocubes,[126] nanorods,[127] or nanotriangles[128]) were successfully determined. The dimensionality of plasmonic nanostructures can also be determined from LSPR spectroscopy,[42–43, 45] which are in excellent agreement with theory[42, 45] thus adding an alternative and fast method for monitoring and quantifying changes in nanoparticle dimensionality.

These measurements have revealed that nanoparticle size stability depends on how nanostructures are synthesized. Whether top-down or bottom-up methods are used, defects and surface energy influence size stability.[5] Bottom-up synthesized materials typically

contain fewer surface defects than top-down fabricated structures;[5, 129] however, fabricated structures are influenced by their support and often have more tunable morphologies and compositions than synthesized ones.

Regardless of the mechanism of growth, nanoparticle size stability is driven by homogeneity of the nanoparticles formed in terms of size, shape, and crystallinity as well as critical size dimensions.[129] Other parameters that influence nanoparticle size stability depend on the density[9, 130] and adsorption energy[44, 131] of surface stabilizing agents. For a constant total surface area for nanostructures, low densities of stabilizing agent leads to large stable nanoparticles over time.[130] This can be understood in terms of maximizing both van der Waals and elastic interaction pair potentials for nanostructures.

Surface chemistry composition can also promote stability in terms of nanoparticle size because of binding energetics. For instance, the preservation of stable Ag nanoparticles with diameters ranging from 44, 39, 35, and 31 nm are observed in the presence of PEG (van der Waals), EDTA (chelate), PVP (covalent-like-N), and PVA (covalent-like-O), respectively.[131] Similar tunability is observed for Au nanostars stabilized by various Good's buffers,[44] as well as metal oxide nanostructures[67, 69] stabilized by zwitterions. In addition, thiol molecules[17, 117] can be used to promote the stability and preservation of size and to improve size distribution. 6-Mercaptohexanoic acid,[49] for example, can limit morphological transformations of gold nanostructures upon adsorption by reducing their effective surface energies. In contrast, dodecanethiol[118] narrowed the size distribution of nanoparticles via digestive ripening. Non-thiolated molecules can also be used for these purposes. Similar effects occur with N-heterocyclic carbenes[132–134] as these adsorb strongly to Au at high temperatures (~373 K) or in dilute H_2O_2. These observations suggest that stabilizing agent composition and structure impacts nanoparticle size stabilization likely through the manipulation of particle surface tension.

All in all, nanoparticle size stability is an important parameter in the observed and exploited physicochemical properties of nanoscale materials. The conservation of dimensionality depends on the homogeneity of the originally synthesized materials[5] as well as stabilizing agents present during storage or use. Size does not typically follow normal distributions. As such, methods deviating from simple averages and standard deviation are encouraged when both quantifying and classifying changes in nanoparticle size.

Stability in Terms of Surface Chemistry.

As conveyed in each of the previous sections, the nanoparticle interface plays an important role in maintaining stability in terms of composition, morphology, and size. Nanomaterials stabilized by their native metal/metal oxide surface atoms require preservation of atomic density, chemical identity, and surface potential while those containing capping agents also rely on properties related to the terminal group protonation state, density, and composition. Instability is noted as variations in surface atomic and molecular density, chemical composition, and potential, which cause unexpected aggregation,[65] irreproducible drug delivery,[135] and inconsistent molecular detection.[46, 136] Altering the surface potential from non-zero values to zero, for instance, reduces the electrostatic repulsive potential between nanoparticles suspended in a medium, an effect that can cause cluster formation. Surface

potential transformations can also influence drug delivery as both drug loading and particle delivery depend on surface potential. As a result, metal/metal oxide surface chemistry stability is important when intermolecular forces influence the use of nanoparticles in applications. While an imperfect technique is because of dependencies on ionic strength and model assumptions,[137] changes in surface potential can be estimated using zeta potential.[17, 46] This is an especially powerful method for characterizing metal oxide nanostructures dispersed in aqueous media as they contain natively oxidized surfaces.[10] Silica[28] and titania[138] particles as well as those composed of metal oxides[139–140] exhibit pH-dependent stabilities because of this native oxide layer as indicated from zeta potential measurements. For instance, zeta potential measurements revealed that silica nanoparticles exhibit stable surface potentials for up to 50 hours in solutions with pH ranging from 5.5–6.5.[21]

Specific information related to the chemical identity, density, and ordering of surface agents is often learned using X-ray photoelectron spectroscopy (XPS) and low energy ion scattering.[141–142] For instance, metal oxidation and trace elements have been identified[141] as well as surface chemistry structure[143] extracted using these methods. To identify surface contamination and defects, low-energy ion scattering[141] is utilized. Furthermore, XPS revealed that the chemical composition and structure of 16-mercaptohexadecanoic acid monolayers on gold nanoparticles[143] change with time. Electron spectra for surface analysis simulations were used to understand the experimental results in terms of monolayer density, thickness, and tilt angle.

Finally, surface sensitive methods such as LSPR and SERS can provide details related to molecular density,[17, 46] identity,[28, 49] orientation,[50, 136] and protonation state of molecules on metals.[46] As described in by the previously reported model for shifts in the extinction maximum wavelength[144] and demonstrated in Figure 4B,[46] the extinction maximum wavelength associated with gold coated silver nanoparticles depends on local refractive index (in this example from varying sucrose concentrations) as well as the presence of a silica protection layer. When a porous silica membrane encapsulates the nanoparticles, surface modification from small thiolated molecules is detected from small spectral variations (Figure 4C), yet no instability of the plasmonic nanoparticles due to aggregation was detected.[46]

It should be noted that techniques that provide chemical information are often influenced by intermolecular interactions.[26] Molecules that readily exchange at an interface[106] as well as those with relatively stronger interactions[145] both reach equilibrium interactions thus providing stable surface chemistries for promoting nanoparticle stability. Concentrations of reagents such as citrate,[146] CTAB,[147] nitrate,[148] and thiolate species[9, 51] must be considered as these can promote nanoparticle instability because of aggregation upon increasing ionic strength[146] while also promoting stability by increasing the elastic interaction potential between structures.[149]

Surface chemistry is very important in promoting nanoparticle stability in non-polar solvents.[71] Mixed ligands on nanoparticle surfaces have been hypothesized to form random, striped, or Janus organizations.[150–151] Random arrangement is most probable when the ligands possess similar chemical and structural properties. Striped ordering has been

reported when two ligands with large differences in volume and/or conformational entropy are included.[151] In contrast, Janus nanoparticles form when two ligands form two separate domains on surfaces.[150] Ligands that lead to the formation of Janus structures likely differ in hydrophobicity such as that between tetradecane-1-thiol (hydrophobic) and 11-amino-1-undecanethiol (hydrophilic).[150] All three ligand organizations and their ordering (or lack there-of) depend on ligand chemical identity, functional group, and packing density. Changes in ordering lead to variations in nanoparticle stability, so the retention of original properties and formation of mixed ligands on the surface influences nanoparticle stabilization especially when suspended in non-polar solvents.

Surface functionalization can reduce the probability of nanostructure aggregation; therefore, stability of this engineered surface chemistry must also be assessed.[49, 51] Surface chemistry stability depends on the rate of molecular adsorption, a process that depends on both flux[28, 50] and preexisting surface chemistry,[152] can be monitored in real-time. For instance, Figure 5[136] illustrates the time-dependent process of thiolate monolayer formation on gold. Porous membranes on SERS substrates,[46] for instance, have been shown to control flux as a function of charge and size[153] and to improve biocompatibility.[154] All in all, surface chemistry stability depends on the nature of atoms or molecules present in the local medium surrounding a nanostructure. These conditions are relevant during storage where exchange can occur as well as in complex environments (i.e., the environment or biological systems) where displacement or encapsulation might take place. Implications of changes are important for nanomaterial performance in various applications. As such, effective stabilization methods should be considered.

4. OUTLOOK AND OPPORTUNITIES

What does nanoparticle stability mean? All in all, this term means many different things but ultimately, plays an important role in defining and maintaining the physicochemical properties of nanostructures for subsequent exploitation in both fundamental and applied studies. Nanoparticle stability is not favored thermodynamically relative to macroscale materials at the same standard conditions. Despite this, these phases do exhibit prolonged stability during relevant time periods. As such, nanoparticles are at best, metastable in comparison to macroscale materials, so this must be considered when exploiting applications with these materials. In general, size dependent property retention is desired for a given period of time, and factors that govern stability can be described in terms of aggregation state, core, surface chemistry, and/or surface composition. Methods that facilitate quantification help define these stabilities or lack thereof.

In this section, we outline four opportunities for better understanding and communicating nanoparticle stability as these materials continue to be exploited in research and technology. First, processes such as oxidation[6] or surface modification[82] of surface atoms is thermodynamically favored and can promote retention of nanometer dimensions yet change the properties of the nanomaterial phase. This is a viable option for promoting some while prohibiting other applications involving nanomaterials. Second, as our ability to control nanoparticle morphology expands, traditional techniques for quantifying fine structural details and size begin to fail. For instance, analysis of complex structures such as nanostars

are difficult to image using traditional two-dimensional electron microscopy imaging.[43] Morphology depends on the orientation of the material with respect to the electron beam. There is an opportunity to develop methods for standardization of size descriptors for such nanoparticles as a function of tip-to-tip distances[49] branch lengths,[44] core radius, numbers of branches, and radius of curvature of the tips.[17] These details significantly impact the physicochemical properties of these materials yet standard and widely available imaging methodologies do not currently allow for this information to be learned in a straight-forward manner.

Homogeneity of nanostructures can complicate the resulting stability of these materials. For instance, ripening can lead to dissolution of small(er) particles and growth of large(r) particles so reporting particle distributions that include small and large outliers are important. Hence, a third opportunity in better assessing and controlling nanomaterial stability is implementing more representative metrics for quantifying size. Typical approaches involve the use of averages and standard deviations in reporting nanoparticle dimensions.[17, 28, 46] While size distributions can follow a Gaussian distribution,[155] a lot of information regarding relatively small or large populations are not communicated. As such, reporting size distributions showing histograms or box and whisker plots is a viable approach for more accurate communication of nanoparticle sizes and distributions.

Finally, many size dependent properties of nanomaterials rely on their unique and size dependent surface energies. This very property, however, leads to instability in terms of aggregation and morphology retention. Hence, there are opportunities for developing new strategies for surface modification of these materials. Novel capping agents of non-spherical nanoparticles would help off-set this high surface energy,[5] could prevent undesired surface chemistry changes,[9, 46] help preserve nanostructure morphology, and increase entropic interaction potentials between nanostructures. This last point would help promote retention of primary nanoparticle states and decrease the probability of aggregation from inelastic collisions.

Overall, the metastability of nanoparticles represents the kinetic trapping of a non-thermodynamically minimized energy state associated with this phase. By defining and better quantifying what is meant by stability, we can be more effective at reproducibly realizing stability-dependent properties ranging from catalytic, electrical, magnetic, mechanical, optical, and thermal. To do so, limitations of current state of the art characterization tools as well as local medium conditions should be considered. The goal of this feature article was to break down stability considerations in terms of aggregation, core composition, shape, size, and surface chemistry. These stability definitions and mechanisms impact size dependent properties in unique ways. By defining these and by outlining how these properties can be measured, we hope that the term “nanoparticle stability” is more clearly conveyed and used realistically as these materials continue to be used in research and society.

ACKNOWLEDGMENTS

The authors are gratefully acknowledge funding from the National Science Foundation, (CHE-1707859) and the National Institute of Environmental Health Sciences of the National Institutes of Health (R01ES027145).

Biographies

Hoa T. Phan is a Ph.D. candidate in the Chemistry Department at the University of Iowa and is studying under the direction of Prof. Amanda J. Haes. He received his B.S. degree in Chemistry from Hanoi University of Science, Vietnam National University. His research focuses on investigating molecular protonation states on plasmonic nanoparticles in order to promote SERS detection of uranyl on polymer substrates.

Amanda J. Haes is a Professor in the Chemistry Department at the University of Iowa. Her research group focuses on a number of key issues related to nanoscience and nanotechnology including understanding nanomaterial fate and stability, measuring and modeling how intermolecular forces influence interfacial phenomena in plasmonics and SERS, as well as applying these materials in biological, chemical, dental, environmental, and radiological applications.

REFERENCES

1. ISO/TS 80004–1:2015 Nanotechnologies -- Vocabulary -- Part 1: Core terms 2015.
2. Schmid G Nanoparticles: From Theory to Application; Wiley-VCH: Germany, 2004.
3. Greeley J; Nørskov KJ; Mavrikakis M Electronic Structure and Catalysis on Metal Surfaces. Annu. Rev. Phys. Chem 2002, 53, 319–348. [PubMed: 11972011]
4. Wieckowski A; Savinova ER; Vayenas CG Catalysis and Electrocatalysis at Nanoparticle Surfaces; CRC Press: New York, 2003.
5. Cao G Nanostructures and Nanomaterials, 2nd ed.; World Scientific London 2011.
6. Levard C; Hotze EM; Lowry GV; Brown GE Environmental Transformations of Silver Nanoparticles: Impact on Stability and Toxicity. Environ. Sci. Technol 2012, 46, 6900–6914. [PubMed: 22339502]
7. Roldan Cuenya B; Behafarid F Nanocatalysis: Size- and Shape-Dependent Chemisorption and Catalytic Reactivity. Surf. Sci. Rep 2015, 70, 135–187.
8. den Breejen JP; Radstake PB; Bezemer GL; Bitter JH; Frøseth V; Holmen A; de Jong KP On the Origin of the Cobalt Particle Size Effects in Fischer−Tropsch Catalysis. JACS 2009, 131, 7197–7203.
9. Pierre MCS; Mackie PM; Roca M; Haes AJ Correlating Molecular Surface Coverage and Solution-Phase Nanoparticle Concentration to Surface-Enhanced Raman Scattering Intensities. J. Phys. Chem. C 2011, 115, 18511–18517.
10. Ivanov MR; Haes AJ Nanomaterial Surface Chemistry Design for Advancements in Capillary Electrophoresis Modes. Analyst 2011, 136, 54–63. [PubMed: 20967383]
11. Haes AJ; Haynes CL; McFarland AD; Schatz GC; Van Duyne RP; Zou S Plasmonic Materials for Surface-Enhanced Sensing and Spectroscopy. MRS Bull 2005, 30, 368–375.

12. Kolhatkar A; Jamison A; Litvinov D; Willson R; Lee T Tuning the Magnetic Properties of Nanoparticles. Int. J. Mol. Sci 2013, 14, 15977–16009. [PubMed: 23912237]
13. He X; Shi H Size and Shape Effects on Magnetic Properties of Ni Nanoparticles. Particuology 2012, 10, 497–502.
14. Jeong U; Teng X; Wang Y; Yang H; Xia Y Superparamagnetic Colloids: Controlled Synthesis and Niche Applications. Adv. Mater 2007, 19, 33–60.
15. Guo D; Xie G; Luo J Mechanical Properties of Nanoparticles: Basics and Applications. J. Phys. D: Appl. Phys 2014, 47, 013001.
16. Wang X; Xu X; Choi S, Thermal SU Conductivity of Nanoparticle - Fluid Mixture. J. Thermophys. Heat Tr 1999, 13, 474–480.
17. Xi W; Phan HT; Haes AJ How To Accurately Predict Solution-Phase Gold Nanostar Stability. Anal. Bioanal. Chem 2018, 410, 6113–6123. [PubMed: 29748758]
18. Narayanan R; El-Sayed MA Effect of Catalysis on the Stability of Metallic Nanoparticles: Suzuki Reaction Catalyzed by PVP-Palladium Nanoparticles. JACS 2003, 125, 8340–8347.
19. Li Y; El-Sayed MA The Effect of Stabilizers on the Catalytic Activity and Stability of Pd Colloidal Nanoparticles in the Suzuki Reactions in Aqueous Solution. J. Phys. Chem. B 2001, 105, 8938–8943.
20. Wang C; Daimon H; Onodera T; Koda T; Sun S A General Approach to the Size- and Shape-Controlled Synthesis of Platinum Nanoparticles and Their Catalytic Reduction of Oxygen. Angew. Chem. Int. Ed 2008, 47, 3588–3591.
21. Kim K-M; Kim HM; Lee W-J; Lee C-W; Kim T.-i.; Lee J-K; Jeong J; Paek S-M; Oh J-M Surface Treatment of Silica Nanoparticles for Stable and Charge-Controlled Colloidal Silica. Int. J. Nanomedicine 2014, 9, 29–40. [PubMed: 25565824]
22. Wijenayaka LA; Ivanov MR; Cheatum CM; Haes AJ Improved Parametrization for Extended Derjaguin, Landau, Verwey, and Overbeek Predictions of Functionalized Gold Nanosphere Stability. J. Phys. Chem. C 2015, 119, 10064–10075.
23. Levard C; Reinsch BC; Michel FM; Oumahi C; Lowry GV; Brown GE Sulfidation Processes of PVP-Coated Silver Nanoparticles in Aqueous Solution: Impact on Dissolution Rate. Environ. Sci. Technol 2011, 45, 5260–5266. [PubMed: 21598969]
24. Serna R; Suárez-García A; Afonso CN; Babonneau D Optical Evidence for Reactive Processes When Embedding Cu Nanoparticles in Al2O3 by Pulsed Laser Deposition. Nanotechnology 2006, 17, 4588–4593. [PubMed: 21727581]
25. Huang C-C; Huang C-H; Kuo IT; Chau L-K; Yang T-S Synthesis of Silica-Coated Gold Nanorod as Raman Tags by Modulating Cetyltrimethylammonium Bromide Concentration. Colloids Surf. Physicochem. Eng. Aspects 2012, 409, 61–68.
26. Xi W; Shrestha BK; Haes AJ Promoting Intra- and Intermolecular Interactions in Surface-Enhanced Raman Scattering. Anal. Chem 2018, 90, 128–143. [PubMed: 29056042]
27. Samanta A; Jana S; Das RK; Chang Y-T Wavelength and Shape Dependent SERS Study to Develop Ultrasensitive Nanotags for Imaging of Cancer Cells. RSC Advances 2014, 4, 12415–12421.
28. Shrestha KB; Haes JA Improving Surface Enhanced Raman Signal Rreproducibility Using Gold-coated Silver Nanospheres Encapsulated in Silica Membranes. J. Opt 2015, 17, 114017.
29. Peter S; Romana Z Formulation and Stability Aspects of Nanosized Solid Drug Delivery Systems. Curr. Pharm. Des 2015, 21, 3148–3157. [PubMed: 26027571]
30. Khan I; Saeed K; Khan I Nanoparticles: Properties, Applications and Toxicities. Arab. J. Chem 2017.
31. Goldstein AN; Echer CM; Alivisatos AP Melting in Semiconductor Nanocrystals. Science 1992, 256, 1425–1427. [PubMed: 17791609]
32. Willets KA; Van Duyne RP Localized Surface Plasmon Resonance Spectroscopy and Sensing. Annu. Rev. Phys. Chem 2007, 58, 267–297. [PubMed: 17067281]
33. Kreibig U; Vollmer M Optical Properties of Metal Clusters; Springer, Berlin, Heidelberg, 1995.

34. Fenger R; Fertitta E; Kirmse H; Thünemann AF; Rademann K Size Dependent Catalysis with CTAB-stabilized Gold Nanoparticles. Phys. Chem. Chem. Phys 2012, 14, 9343–9349. [PubMed: 22549475]
35. Lu Y; Mei Y; Walker R; Ballauff M; Drechsler M 'Nano-Tree'—Type Spherical Polymer Brush Particles as Templates for Metallic Nanoparticles. Polymer 2006, 47, 4985–4995.
36. Reske R; Mistry H; Behafarid F; Roldan Cuenya B; Strasser P Particle Size Effects in the Catalytic Electroreduction of CO2 on Cu Nanoparticles. JACS 2014, 136, 6978–6986.
37. Panigrahi S; Basu S; Praharaj S; Pande S; Jana S; Pal A; Ghosh SK; Pal T Synthesis and Size-Selective Catalysis by Supported Gold Nanoparticles: Study on Heterogeneous and Homogeneous Catalytic Process. J. Phys. Chem. C 2007, 111, 4596–4605.
38. Sankar M; Dimitratos N; Miedziak PJ; Wells PP; Kiely CJ; Hutchings GJ Designing Bimetallic Catalysts for A Green and Sustainable Future. Chem. Soc. Rev 2012, 41, 8099–8139. [PubMed: 23093051]
39. Wei Z; Sun J; Li Y; Datye AK; Wang Y Bimetallic catalysts for hydrogen generation. Chem. Soc. Rev 2012, 41, 7994–8008. [PubMed: 23011345]
40. McCrea K; Parker JS; Chen P; Somorjai G Surface Structure Sensitivity of High-Pressure Co Dissociation On Pt(557), Pt(100), and Pt(111) using Sum Frequency Generation Surface Vibrational Spectroscopy. Surf. Sci 2001, 494, 238–250.
41. Hong S; Li X Optimal Size of Gold Nanoparticles for Surface-Enhanced Raman Spectroscopy under Different Conditions. J. Nanomater 2013, 790323.
42. Paramelle D; Sadovoy A; Gorelik S; Free P; Hobley J; Fernig DG A Rapid Method to Estimate the Concentration of Citrate Capped Silver Nanoparticles From UV-Visible Light Spectra. Analyst 2014, 139, 4855–4861. [PubMed: 25096538]
43. de Puig H; Tam JO; Yen C-W; Gehrke L; Hamad-Schifferli K Extinction Coefficient of Gold Nanostars. J. Phys. Chem. C 2015, 119, 17408–17415.
44. Chandra K; Culver KSB; Werner SE; Lee RC; Odom TW Manipulating the Anisotropic Structure of Gold Nanostars using Good's Buffers. Chem. Mater 2016, 28, 6763–6769.
45. Liu X; Atwater M; Wang J; Huo Q Extinction Coefficient of Gold Nanoparticles with Different Sizes and Different Capping Ligands. Colloids Surf., B 2007, 58, 3–7.
46. Phan HT; Haes AJ Impacts of pH and Intermolecular Interactions on Surface-Enhanced Raman Scattering Chemical Enhancements. J. Phys. Chem. C 2018, 122, 14846–14856.
47. Haes AJ; Van Duyne RP A Nanoscale Optical Biosensor: Sensitivity and Selectivity of an Approach Based on the Localized Surface Plasmon Resonance Spectroscopy of Triangular Silver Nanoparticles. JACS 2002, 124, 10596–10604.
48. Nikoobakht B; El-Sayed MA Preparation and Growth Mechanism of Gold Nanorods (NRs) Using Seed-Mediated Growth Method. Chem. Mater 2003, 15, 1957–1962.
49. Lu G; Forbes TZ; Haes AJ SERS Detection of Uranyl Using Functionalized Gold Nanostars Promoted by Nanoparticle Shape and Size. Analyst 2016, 141, 5137–5143. [PubMed: 27326897]
50. Lu G; Shrestha B; Haes AJ Importance of Tilt Angles of Adsorbed Aromatic Molecules on Nanoparticle Rattle SERS Substrates. J. Phys. Chem. C 2016, 120, 20759–20767.
51. Volkert AA; Subramaniam V; Ivanov MR; Goodman AM; Haes AJ Salt-Mediated Self-Assembly of Thioctic Acid on Gold Nanoparticles. ACS Nano 2011, 5, 4570–4580. [PubMed: 21524135]
52. Guardia P; Labarta A; Batlle X Tuning the Size, the Shape, and the Magnetic Properties of Iron Oxide Nanoparticles. J. Phys. Chem. C 2011, 115, 390–396.
53. Broitman E Indentation Hardness Measurements at Macro-, Micro-, and Nanoscale: A Critical Overview. Tribol. Lett 2016, 65, 23.
54. Ramos MO-J,L; Hurtado-Macias A; Flores S; Elizalde-Galindo JT; Rocha C; Torres B; Zarei-Chaleshtori M; Chianelli RR Hardness and Elastic Modulus on Six-Fold Symmetry Gold Nanoparticles. Materials 2013, 6, 198–205. [PubMed: 28809302]
55. Hansen N Hall–Petch Relation and Boundary Strengthening. Scripta Mater 2004, 51, 801–806.
56. Zhang N; Deng Q; Hong Y; Xiong L; Li S; Strasberg M; Yin W; Zou Y; Taylor CR; Sawyer G, et al. Deformation Mechanisms in Silicon Nanoparticles. J. Appl. Phys 2011, 109, 063534.

57. Guo D; Li J; Chang L; Luo J Measurement of the Friction between Single Polystyrene Nanospheres and Silicon Surface Using Atomic Force Microscopy. Langmuir 2013, 29, 6920–6925. [PubMed: 23725519]
58. Heim L-O; Blum J; Preuss M; Butt H-J Adhesion and Friction Forces between Spherical Micrometer-Sized Particles. Phys. Rev. Lett 1999, 83, 3328–3331.
59. Salameh S; Schneider J; Laube J; Alessandrini A; Facci P; Seo JW; Ciacchi LC; Mädler L Adhesion Mechanisms of the Contact Interface of TiO2 Nanoparticles in Films and Aggregates. Langmuir 2012, 28, 11457–11464. [PubMed: 22780850]
60. Kappl M; Butt H-J The Colloidal Probe Technique and its Application to Adhesion Force Measurements. Part. Part. Syst. Charact 2002, 19, 129–143.
61. Carrillo J-MY; Raphael E; Dobrynin AV Adhesion of Nanoparticles. Langmuir 2010, 26, 12973–12979. [PubMed: 20602529]
62. Iyahraja S; Rajadurai JS Study of Thermal Conductivity Enhancement of Aqueous Suspensions Containing Silver Nanoparticles. AIP Advances 2015, 5, 057103.
63. Kim HJ; Lee S-H; Kim SB; Jang SP The Effect of Nanoparticle Shape on The Thermal Resistance of A Flat-Plate Heat Pipe Using Acetone-Based Al2O3 Nanofluids. Int. J. Heat Mass Transf 2016, 92, 572–577.
64. Do KH; Jang SP Effect of Nanofluids on The Thermal Performance of A Flat Micro Heat Pipe with A Rectangular Grooved Wick. Int. J. Heat Mass Transf 2010, 53, 2183–2192.
65. Hotze EM; Phenrat T; Lowry GV Nanoparticle Aggregation: Challenges to Understanding Transport and Reactivity in the Environment. J. Environ. Qual 2010, 39, 1909–1924. [PubMed: 21284288]
66. Murphy RJ; Pristinski D; Migler K; Douglas JF; Prabhu VM Dynamic Light Scattering Investigations of Nanoparticle Aggregation Following A Light-Induced pH Jump. J. Chem. Phys 2010, 132, 194903. [PubMed: 20499988]
67. Keller AA; Wang H; Zhou D; Lenihan HS; Cherr G; Cardinale BJ; Miller R; Ji Z Stability and Aggregation of Metal Oxide Nanoparticles in Natural Aqueous Matrices. Environ. Sci. Technol 2010, 44, 1962–1967. [PubMed: 20151631]
68. McNaught AD; Wilkinson A IUPAC. Compendium of Chemical Terminology, 2nd ed. (the “Gold Book”); Wiley Blackwell, 2014.
69. Singh LP; Bhattacharyya SK; Mishra G; Ahalawat S Functional Role of Cationic Surfactant to Control The Nano Size of Silica Powder. Appl. Nanosci 2011, 1, 117–122.
70. Wagers KB; Chui TCP; Adem S Effect of pH on the Stability of Gold Nanoparticles and Their Application for Melamine Detection in Infant Formula. IOSR-JAC 2014, 7, 15–20.
71. Yang Y; Qin H; Jiang M; Lin L; Fu T; Dai X; Zhang Z; Niu Y; Cao H; Jin Y, et al. Entropic Ligands for Nanocrystals: From Unexpected Solution Properties to Outstanding Processability. Nano Lett 2016, 16, 2133–2138. [PubMed: 26923682]
72. Yin Y; Li Z-Y; Zhong Z; Gates B; Xia Y; Venkateswaran S Synthesis and Characterization of Stable Aqueous Dispersions of Silver Nanoparticles through The Tollens Process. J. Mater. Chem 2002, 12, 522–527.
73. Han J; Liu W; Zhang T; Xue K; Li W; Jiao F; Qin W Mechanism Study on The Sulfidation of ZnO With Sulfur and Iron Oxide at High Temperature. Sci. Rep 2017, 7, 42536–42536. [PubMed: 28186156]
74. Ma R; Levard C; Michel FM; Brown GE; Lowry GV Sulfidation Mechanism for Zinc Oxide Nanoparticles and the Effect of Sulfidation on Their Solubility. Environ. Sci. Technol 2013, 47, 2527–2534. [PubMed: 23425191]
75. Rahman SSU; Qureshi MT; Sultana K; Rehman W; Khan MY; Asif MH; Farooq M; Sultana N Single Step Growth of Iron Oxide Nanoparticles and Their Use as Glucose Biosensor. Results Phys 2017, 7, 4451–4456.
76. Ruíz-Baltazar A; Esparza R; Rosas G; Pérez R Effect of the Surfactant on the Growth and Oxidation of Iron Nanoparticles. J. Nanomater 2015, 2015, 8.
77. Martina I; Wiesinger R; Jembrih-Simburger D; Schreiner M Micro-Raman Characterization of Silver Corrosion Products: Instrumental Set-Up and Reference Database; Morana RTD d.o.o., 2012.

78. Goldstein J; Newbury DE; Joy DC; Echlin P; Lyman CE; Lifshin E; Sawyer L; Micheal J Scanning Electron Microscopy and X-Ray Microanalysis: Third Edition; Springer US, 2003.
79. Scimeca M; Bischetti S; Lamsira HK; Bonfiglio R; Bonanno E Energy Dispersive X-ray (EDX) Microanalysis: A Powerful Tool in Biomedical Research and Diagnosis. Eur. J. Histochem 2018, 62, 2841–2841. [PubMed: 29569878]
80. Russ JC Fundamentals of Energy Dispersive X-ray Analysis; Butterworths, 1984.
81. Uemura Y; Inada Y; Niwa Y; Kimura M; Bando KK; Yagishita A; Iwasawa Y; Nomura M Formation and Oxidation Mechanisms of Pd–Zn Nanoparticles on a ZnO Supported Pd Catalyst Studied By In Situ Time-Resolved QXAFS and DXAFS. Phys. Chem. Chem. Phys 2012, 14, 2152–2158. [PubMed: 21997731]
82. Noor F; Zhang H; Korakianitis T; Wen D Oxidation and Ignition of Aluminum Nanomaterials. Phys. Chem. Chem. Phys 2013, 15, 20176–20188. [PubMed: 24162275]
83. Chen C-H; Yamaguchi T; Sugawara K.-i.; Koga K Role of Stress in the Self-Limiting Oxidation of Copper Nanoparticles. J. Phys. Chem. B 2005, 109, 20669–20672. [PubMed: 16853677]
84. Eidelman KB; Tabachkova NY; Shcherbachev KD; Parkhomenko YN; Privesentsev VV; Migunov DM Structural Properties of The Formation of Zinc-Containing Nanoparticles Obtained by Ion Implantation in Si (001) and Subsequent Thermal Annealing. Mod. Electron. Mater 2017, 3, 104–109.
85. Yathindranath V; Worden M; Sun Z; Miller DW; Hegmann T A General Synthesis of Metal (Mn, Fe, Co, Ni, Cu, Zn) Oxide and Silica Nanoparticles Based on A Low Temperature Reduction/Hydrolysis Pathway. RSC Advances 2013, 3, 23722–23729.
86. Chen M; Wang L-Y; Han J-T; Zhang J-Y; Li Z-Y; Qian D-J Preparation and Study of Polyacryamide-Stabilized Silver Nanoparticles through a One-Pot Process. J. Phys. Chem. B 2006, 110, 11224–11231. [PubMed: 16771388]
87. Fang C; Lee YH; Shao L; Jiang R; Wang J; Xu Q-H Correlating the Plasmonic and Structural Evolutions during the Sulfidation of Silver Nanocubes. ACS Nano 2013, 7, 9354–9365. [PubMed: 24032644]
88. Lide DR CRC Handbook of Chemistry and Physics; CRC Press: Boca Raton, 2009.
89. Kubaschewski O; von Goldbeck O The Thermochemistry of Gold. Gold Bulletin 1975, 8, 80–85.
90. Ivanova OS; Zamborini FP Size-Dependent Electrochemical Oxidation of Silver Nanoparticles. JACS 2010, 132, 70–72.
91. Li Y; Zhang H; Wu B; Guo Z Improving The Oxidation Resistance And Stability Of Ag Nanoparticles By Coating With Multilayered Reduced Graphene Oxide. Appl. Surf. Sci 2017, 425, 194–200.
92. Liu Z; Yang Y; Liang J; Hu Z; Li S; Peng S; Qian Y Synthesis of Copper Nanowires via a Complex-Surfactant-Assisted Hydrothermal Reduction Process. J. Phys. Chem. B 2003, 107, 12658–12661.
93. Kim NR; Shin K; Jung I; Shim M; Lee HM Ag–Cu Bimetallic Nanoparticles with Enhanced Resistance to Oxidation: A Combined Experimental and Theoretical Study. J. Phys. Chem. C 2014, 118, 26324–26331.
94. Yin Y; Rioux RM; Erdonmez CK; Hughes S; Somorjai GA; Alivisatos AP Formation of Hollow Nanocrystals Through the Nanoscale Kirkendall Effect. Science 2004, 304, 711–714. [PubMed: 15118156]
95. González E; Arbiol J; Puntes VF Carving at the Nanoscale: Sequential Galvanic Exchange and Kirkendall Growth at Room Temperature. Science 2011, 334, 1377–1380. [PubMed: 22158813]
96. Sun Y; Xia Y Alloying and Dealloying Processes Involved in the Preparation of Metal Nanoshells through a Galvanic Replacement Reaction. Nano Lett 2003, 3, 1569–1572.
97. Smigelskas AD; Kirkendall EO Zinc Diffusion in Alpha Brass. Trans. AIME 1947, 171, 130–142.
98. Zapata-Urzúa C; Pérez-Ortiz M; Acosta GA; Mendoza J; Yedra L; Estradé S; Álvarez-Lueje A; Núñez-Vergara LJ; Albericio F; Lavilla R, et al. Hantzsch Dihydropyridines: Privileged Structures for the Formation of Well-defined Gold Nanostars. J. Colloid Interface Sci 2015, 453, 260–269. [PubMed: 25989057]
99. Huang C-J; Chiu P-H; Wang Y-H; Chen WR; Meen TH Synthesis of the Gold Nanocubes by Electrochemical Technique. J. Electrochem. Soc 2006, 153, D129–D133.

100. Wang ZL; Gao RP; Nikoobakht B; El-Sayed MA Surface Reconstruction of the Unstable {110} Surface in Gold Nanorods. J. Phys. Chem. B 2000, 104, 5417–5420.
101. Motzkus C; Macé T; Gaie-Levrel F; Ducourtieux S; Delvallee A; Dirscherl K; Hodoroaba V-D; Popov I; Popov O; Kuselman I, et al. Size Characterization of Airborne SiO2 Nanoparticles with On-Line and Off-Line Measurement Techniques: An Interlaboratory Comparison Study. J. Nanopart. Res 2013, 15, 1919.
102. Ding Y; Gao Y; Wang ZL; Tian N; Zhou Z-Y; Sun S-G Facets and Surface Relaxation of Tetrahexahedral Platinum Nanocrystals. Appl. Phys. Lett 2007, 91, 121901.
103. Martin DC; Thomas EL Experimental High-resolution Electron Microscopy of Polymers. Polymer 1995, 36, 1743–1759.
104. Bhatta UM; Ross IM; Sayle TXT; Sayle DC; Parker SC; Reid D; Seal S; Kumar A; Möbus G Cationic Surface Reconstructions on Cerium Oxide Nanocrystals: An Aberration-Corrected HRTEM Study. ACS Nano 2012, 6, 421–430. [PubMed: 22148265]
105. Link S; Mohamed MB; El-Sayed MA Simulation of the Optical Absorption Spectra of Gold Nanorods as a Function of Their Aspect Ratio and the Effect of the Medium Dielectric Constant. J. Phys. Chem. B 1999, 103, 3073–3077.
106. Park J-W; Shumaker-Parry JS Structural Study of Citrate Layers on Gold Nanoparticles: Role of Intermolecular Interactions in Stabilizing Nanoparticles. JACS 2014, 136, 1907–1921.
107. Huang H; Yang X Synthesis of Chitosan-Stabilized Gold Nanoparticles in the Absence/Presence of Tripolyphosphate. Biomacromolecules 2004, 5, 2340–2346. [PubMed: 15530050]
108. Huo Z; Tsung C.-k.; Huang W; Zhang X; Yang P Sub-Two Nanometer Single Crystal Au Nanowires. Nano Lett 2008, 8, 2041–2044. [PubMed: 18537294]
109. Desireddy A; Conn BE; Guo J; Yoon B; Barnett RN; Monahan BM; Kirschbaum K; Griffith WP; Whetten RL; Landman U, et al. Ultrastable Silver Nanoparticles. Nature 2013, 501, 399. [PubMed: 24005327]
110. Klajn R; Pinchuk AO; Schatz GC; Grzybowski BA Synthesis of Heterodimeric Sphere–Prism Nanostructures via Metastable Gold Supraspheres. Angew. Chem. Int. Ed 2007, 46, 8363–8367.
111. Udayabhaskararao T; Altantzis T; Houben L; Coronado-Puchau M; Langer J; Popovitz-Biro R; Liz-Marzán LM; Vuković L; Král P; Bals S, et al. Tunable Porous Nanoallotropes Prepared by Post-assembly Etching of Binary Nanoparticle Superlattices. Science 2017, 358, 514–518. [PubMed: 29074773]
112. Zheng Y; Zeng J; Ruditskiy A; Liu M; Xia Y Oxidative Etching and Its Role in Manipulating the Nucleation and Growth of Noble-Metal Nanocrystals. Chem. Mater 2014, 26, 22–33.
113. Wiley B; Herricks T; Sun Y; Xia Y Polyol Synthesis of Silver Nanoparticles: Use of Chloride and Oxygen to Promote the Formation of Single-Crystal, Truncated Cubes and Tetrahedrons. Nano Lett 2004, 4, 1733–1739.
114. Xi W; Haes AJ Elucidation of HEPES Affinity to and Structure on Gold Nanostars. JACS 2019, 141, 4034–4042.
115. Koczkur KM; Mourdikoudis S; Polavarapu L; Skrabalak SE Polyvinylpyrrolidone (PVP) in Nanoparticle Synthesis. Dalton Trans 2015, 44, 17883–17905. [PubMed: 26434727]
116. Manson J; Kumar D; Meenan BJ; Dixon D Polyethylene Glycol Functionalized Gold Nanoparticles: The Influence of Capping Density on Stability in Various Media. Gold Bulletin 2011, 44, 99–105.
117. Stoeva SI; Zaikovski V; Prasad BLV; Stoimenov PK; Sorensen CM; Klabunde KJ Reversible Transformations of Gold Nanoparticle Morphology. Langmuir 2005, 21, 10280–10283. [PubMed: 16262276]
118. Stoeva S; Klabunde KJ; Sorensen CM; Dragieva I Gram-Scale Synthesis of Monodisperse Gold Colloids by the Solvated Metal Atom Dispersion Method and Digestive Ripening and Their Organization into Two- and Three-Dimensional Structures. JACS 2002, 124, 2305–2311.
119. Rigden JS Macmillan Encyclopedia of Physics: S-Z. Index; Simon & Schuster Macmillan: New York, 1996.
120. Kranz C; Mizaikoff B In Comprehensive Analytical Chemistry, Valcárcel M; López-Lorente ÁI, Eds. Elsevier: 2014; Vol. 66, pp 257–299.

121. Hoo CM; Starostin N; West P; Mecartney ML A Comparison of Atomic Force Microscopy (AFM) and Dynamic Light Scattering (DLS) Methods to Characterize Nanoparticle Size Distributions. J. Nanopart. Res 2008, 10, 89–96.

122. Bhushan B; Marti O In Nanotribology and Nanomechanics: An Introduction, Bhushan B, Ed. Springer Berlin Heidelberg: Berlin, Heidelberg, 2005; pp 41–115.

123. Li T; Senesi AJ; Lee B Small Angle X-ray Scattering for Nanoparticle Research. Chem. Rev 2016, 116, 11128–11180. [PubMed: 27054962]

124. Miller CC The Stokes-Einstein Law for Diffusion in Solution. Proc. R. Soc. London, Ser. A 1924, 106, 724–749.

125. Polte J; Ahner TT; Delissen F; Sokolov S; Emmerling F; Thünemann AF; Kraehnert R Mechanism of Gold Nanoparticle Formation in the Classical Citrate Synthesis Method Derived from Coupled In Situ XANES and SAXS Evaluation. JACS 2010, 132, 1296–1301.

126. Li R; Bian K; Wang Y; Xu H; Hollingsworth JA; Hanrath T; Fang J; Wang Z An Obtuse Rhombohedral Superlattice Assembled by Pt Nanocubes. Nano Lett 2015, 15, 6254–6260. [PubMed: 26280872]

127. Gómez-Graña S; Hubert F; Testard F; Guerrero-Martínez A; Grillo I; Liz-Marzán LM; Spalla O Surfactant (Bi)Layers on Gold Nanorods. Langmuir 2012, 28, 1453–1459. [PubMed: 22165910]

128. Kuttner C; Mayer M; Dulle M; Moscoso A; López-Romero JM; Förster S; Fery A; Pérez-Juste J; Contreras-Cáceres R Seeded Growth Synthesis of Gold Nanotriangles: Size Control, SAXS Analysis, and SERS Performance. ACS Anal. Mater. Interfaces 2018, 10, 11152–11163.

129. Park J; Joo J; Kwon SG; Jang Y; Hyeon T Synthesis of Monodisperse Spherical Nanocrystals. Angew. Chem. Int. Ed 2007, 46, 4630–4660.

130. He B; Tan JJ; Liew KY; Liu H Synthesis of Size Controlled Ag Nanoparticles. J. Mol. Catal. A: Chem 2004, 221, 121–126.

131. Ajitha B; Kumar Reddy YA; Reddy PS; Jeon H-J; Ahn CW Role of Capping Agents In Controlling Silver Nanoparticles Size, Antibacterial Activity And Potential Application As Optical Hydrogen Peroxide Sensor. RSC Advances 2016, 6, 36171–36179.

132. MacLeod MJ; Johnson JA PEGylated N-Heterocyclic Carbene Anchors Designed To Stabilize Gold Nanoparticles in Biologically Relevant Media. JACS 2015, 137, 7974–7977.

133. Salorinne K; Man RWY; Li C-H; Taki M; Nambo M; Crudden CM Water-Soluble N-Heterocyclic Carbene-Protected Gold Nanoparticles: Size-Controlled Synthesis, Stability, and Optical Properties. Angew. Chem. Int. Ed 2017, 56, 6198–6202.

134. Crudden CM; Horton JH; Ebralidze II; Zenkina OV; McLean AB; Drevniok B; She Z; Kraatz H-B; Mosey NJ; Seki T, et al. Ultra Stable Self-assembled Monolayers of N-Heterocyclic Carbenes on Gold. Nat. Chem 2014, 6, 409. [PubMed: 24755592]

135. Singh R; Lillard JW Nanoparticle-based Targeted Drug Delivery. Exp. Mol. Pathol 2009, 86, 215–223. [PubMed: 19186176]

136. Wang X; Zhong JH; Zhang M; Liu Z; Wu DY; Ren B Revealing Intermolecular Interaction and Surface Restructuring of an Aromatic Thiol Assembling on Au(111) by Tip-Enhanced Raman Spectroscopy. Anal. Chem 2016, 88, 915–921. [PubMed: 26633597]

137. Ohshima H Electrostatic Interaction between a Hard Sphere with Constant Surface Charge Density and a Soft Sphere: Polarization Effect of a Hard Sphere. J. Colloid Interface Sci 1994, 168, 255–265.

138. McNamee CE; Tsujii Y; Matsumoto M Physicochemical Characterization of an Anatase TiO2 Surface and the Adsorption of a Nonionic Surfactant: An Atomic Force Microscopy Study. Langmuir 2005, 21, 11283–11288. [PubMed: 16285801]

139. Cuddy MF; Poda AR; Brantley LN Determination of Isoelectric Points and the Role of pH for Common Quartz Crystal Microbalance Sensors. ACS Anal. Mater. Interfaces 2013, 5, 3514–3518.

140. Kittaka S Isoelectric Point of Al_2O_3, Cr_2O_3 and Fe_2O_3. II. Binary Solid Solution. J. Colloid Interface Sci 1974, 48, 334–338.

141. Baer DR; Engelhard MH; Johnson GE; Laskin J; Lai J; Mueller K; Munusamy P; Thevuthasan S; Wang H; Washton N, et al. Surface Characterization of Nanomaterials and Nanoparticles:

Important Needs and Challenging Opportunities. J. Vac. Sci. Technol. A 2013, 31, 50820–50820. [PubMed: 24482557]

142. Powell CJ Growth and Trends in Auger-Electron Spectroscopy and X-Ray Photoelectron Spectroscopy for Surface Analysis. J. Vac. Sci. Technol. A 2003, 21, S42–S53.
143. Techane S; Baer DR; Castner DG Simulation and Modeling of Self-Assembled Monolayers of Carboxylic Acid Thiols on Flat and Nanoparticle Gold Surfaces. Anal. Chem 2011, 83, 6704–6712. [PubMed: 21744862]
144. Haes AJ; Zou S; Schatz GC; Van Duyne RP A Nanoscale Optical Biosensor: The Long Range Distance Dependence of the Localized Surface Plasmon Resonance of Noble Metal Nanoparticles. J. Phys. Chem. B 2004, 108, 109–116.
145. Burgi T Properties of the Gold-Sulphur Interface: from Self-Assembled Monolayers to Clusters. Nanoscale 2015, 7, 15553–15567. [PubMed: 26360607]
146. Henglein A; Giersig M Formation of Colloidal Silver Nanoparticles: Capping Action of Citrate. J. Phys. Chem. B 1999, 103, 9533–9539.
147. Rostro-Kohanloo BC; Bickford LR; Payne CM; Day ES; Anderson LJE; Zhong M; Lee S; Mayer KM; Zal T; Adam L, et al. The Stabilization and Targeting of Surfactant-Synthesized Gold Nanorods. Nanotechnology 2009, 20, 434005. [PubMed: 19801751]
148. Pamies R; Cifre JGH; Espín VF; Collado-González M; Baños FGD; de la Torre JG Aggregation Behaviour of Gold Nanoparticles in Saline Aqueous Media. J. Nanopart. Res 2014, 16, 2376.
149. Gorham JM; Rohlfing AB; Lippa KA; MacCuspie RI; Hemmati A; David Holbrook R Storage Wars: How Citrate-Capped Silver Nanoparticle Suspensions are Affected by Not-So-Trivial Decisions. J. Nanopart. Res 2014, 16, 2339.
150. Kim H; Carney RP; Reguera J; Ong QK; Liu X; Stellacci F Synthesis and Characterization of Janus Gold Nanoparticles. Adv. Mater 2012, 24, 3857–3863. [PubMed: 22573487]
151. Velachi V; Bhandary D; Singh JK; Cordeiro MNDS Striped Gold Nanoparticles: New Insights from Molecular Dynamics Simulations. J. Chem. Phys 2016, 144, 244710. [PubMed: 27369536]
152. Gooßen LJ; Thiel WR; Rodríguez N; Linder C; Melzer B Copper-Catalyzed Protodecarboxylation of Aromatic Carboxylic Acids. Adv. Synth. Catal 2007, 349, 2241–2246.
153. Zdravkov BD; Čermák JJ; Šefara M; Janků J Pore Classification in The Characterization of Porous Materials: A Perspective. Cent. Eur. J. Chem 2007, 5, 385–395.
154. Fabris L Gold-based SERS Tags for Biomedical Imaging. J. Opt 2015, 17, 114002.
155. Bienert R; Emmerling F; Thünemann AF The Size Distribution of ‘Gold Standard’ Nanoparticles. Anal. Bioanal. Chem 2009, 395, 1651. [PubMed: 19756546]

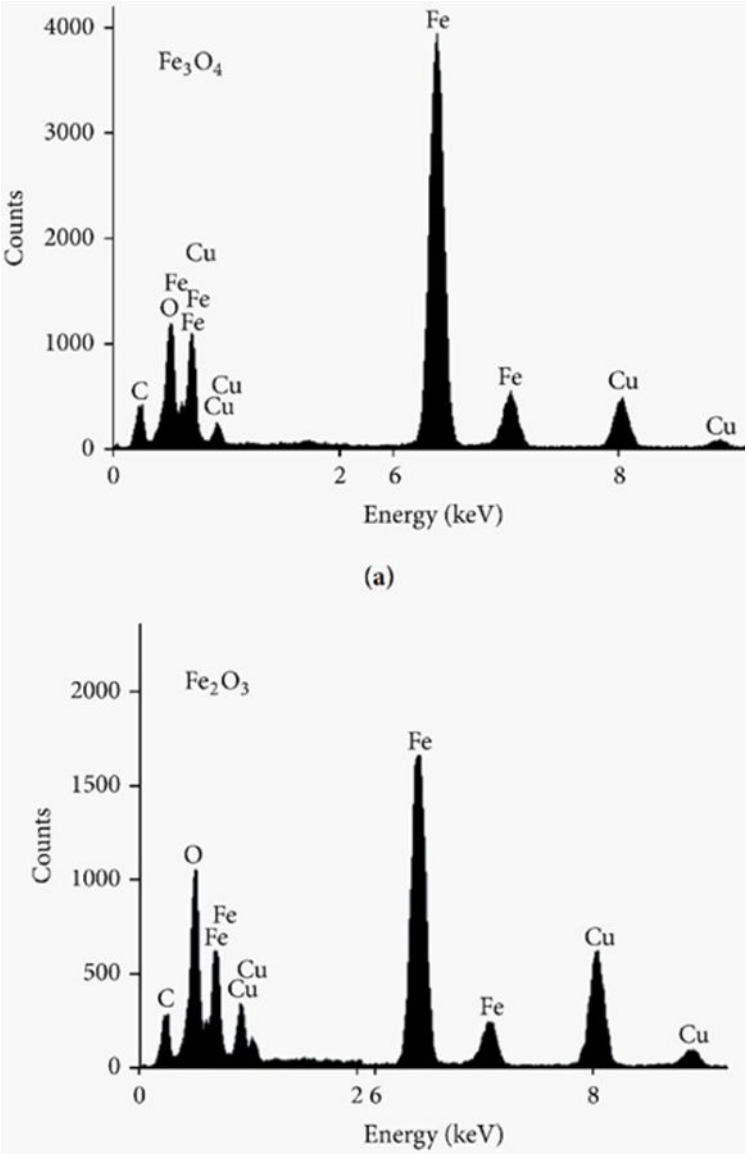

Figure 1.
EDS spectra of (top) Fe_3O_4 and (bottom) Fe_2O_3 nanoparticles.[76]

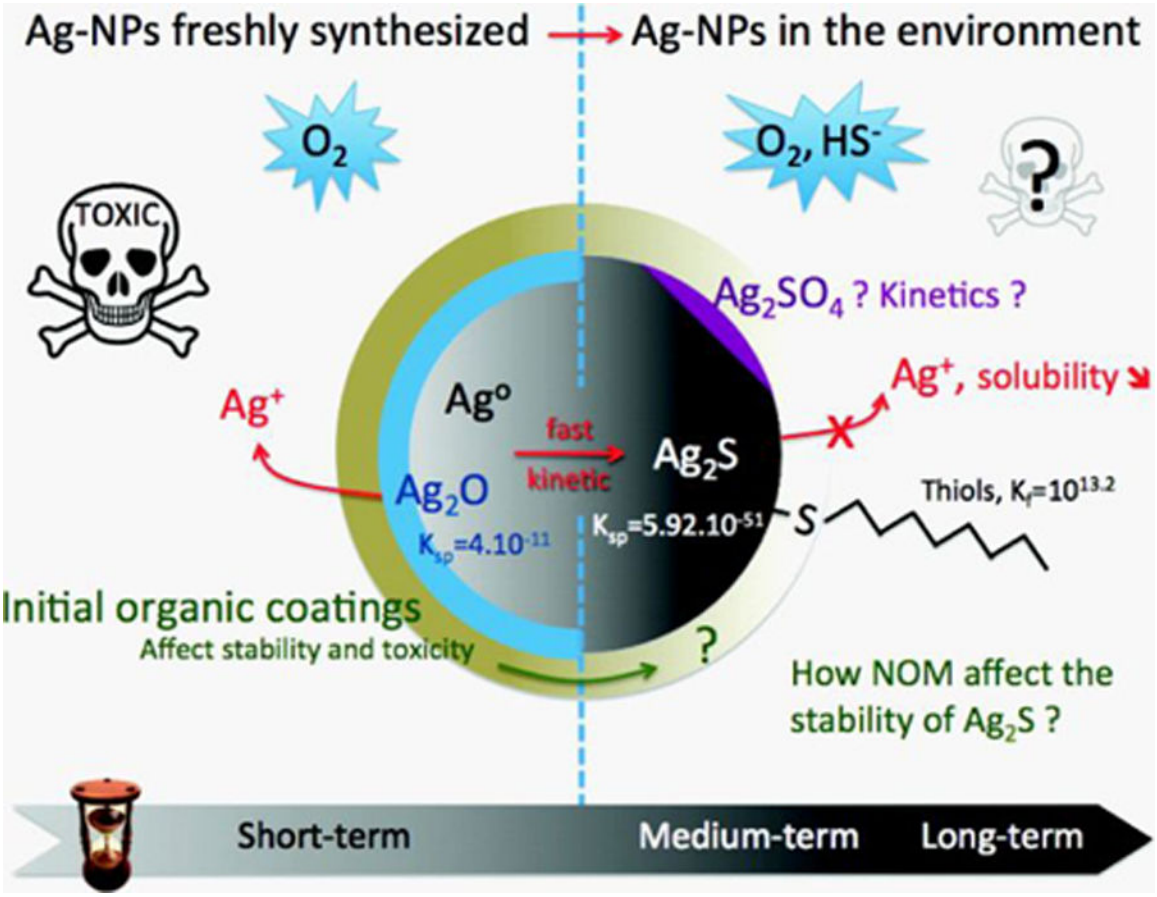

Figure 2.
Transformations of silver nanoparticle cores in the environment. Reprinted with permission from ref 6. Copyright 2012 American Chemical Society.

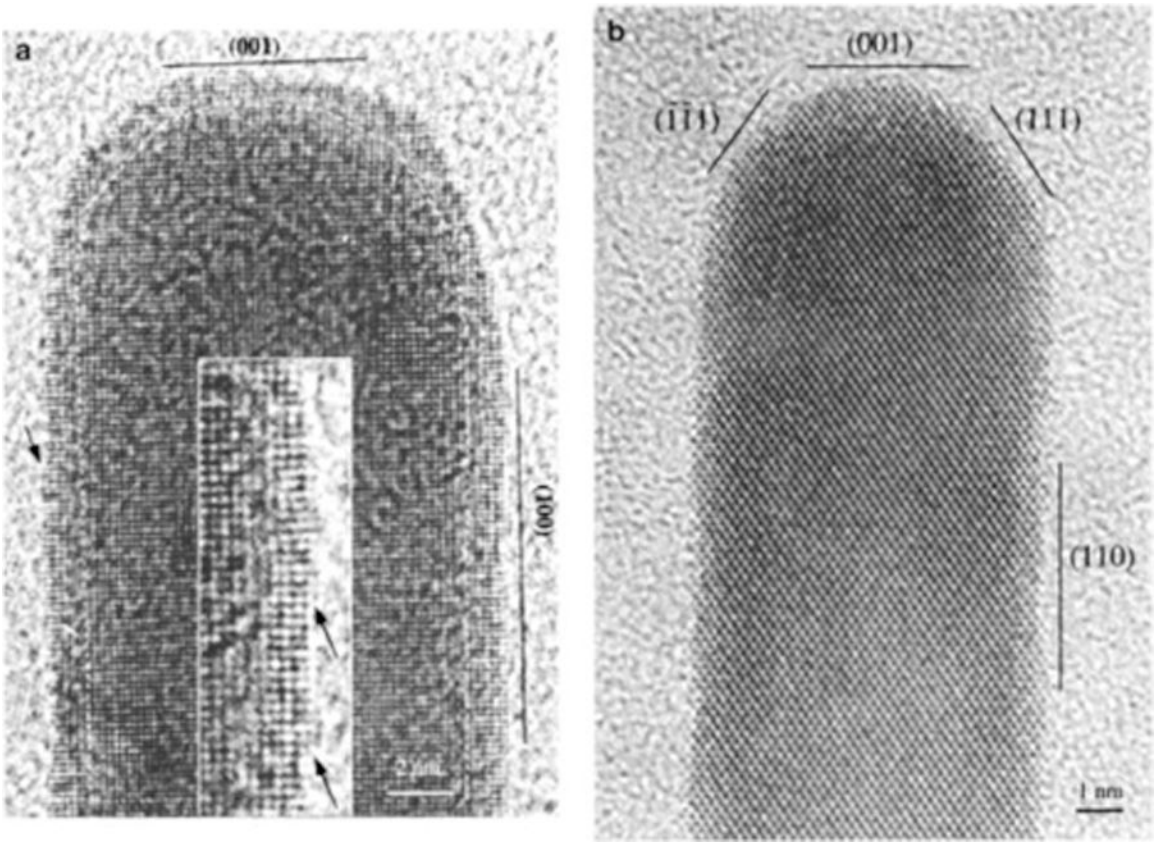

Figure 3.
HR-TEM images of the Au nanorods with facets oriented along (a) (010) and (b) (110) planes. Reprinted with permission from ref 100. Copyright 2000 American Chemical Society.

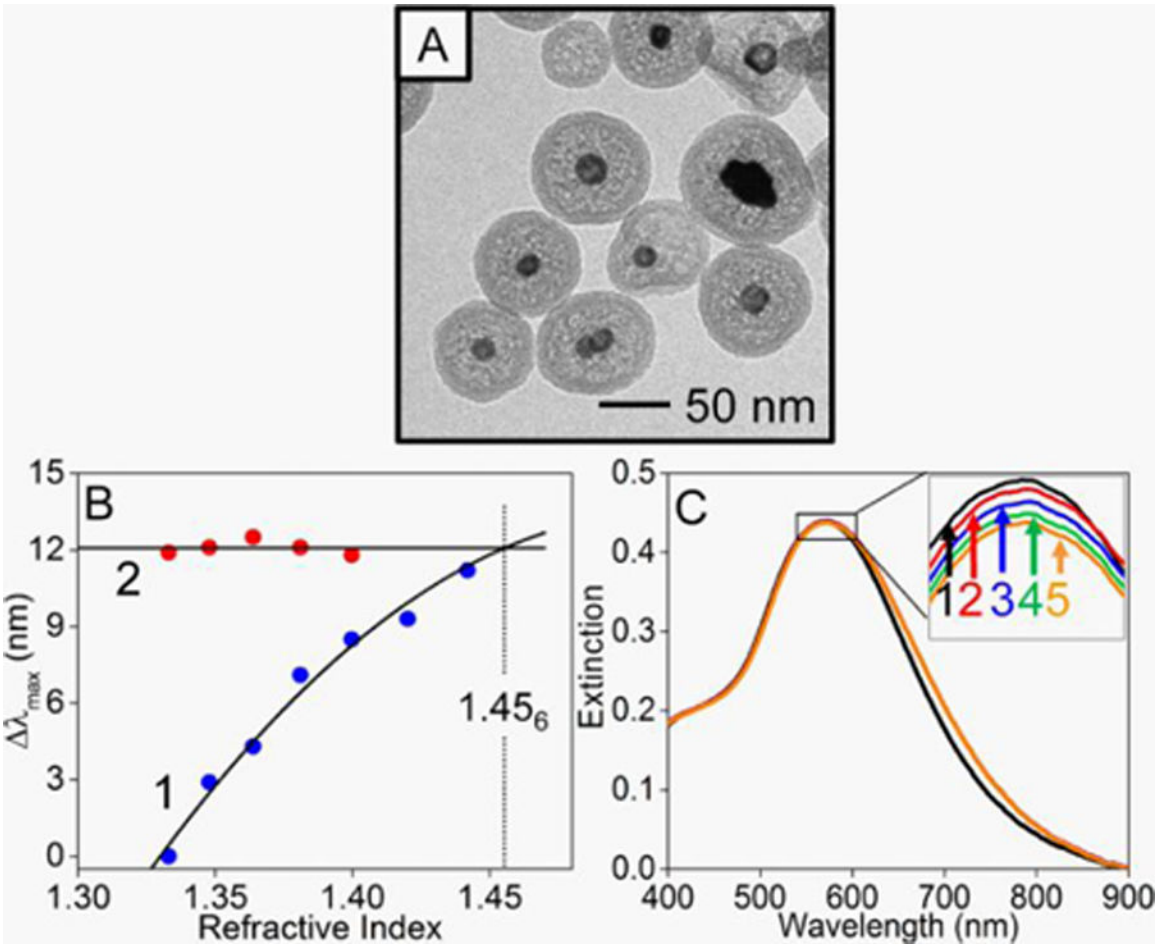

Figure 4.

(A) TEM image of internally etched Ag@Au@SiO_2 nanoparticles. (B) Changes in extinction maximum wavelength from LSPR spectra (1) without and (2) with silica membranes as a function of bulk refractive index. (C) LSPR spectra of the same materials (1) before and after incubation with 4-mercaptobenzoic acid in pH 4.5 buffer for (2) 1, (3) 10, (4) 30, and (5) 45 minutes. Reprinted with permission from ref 46. Copyright 2018 American Chemical Society.

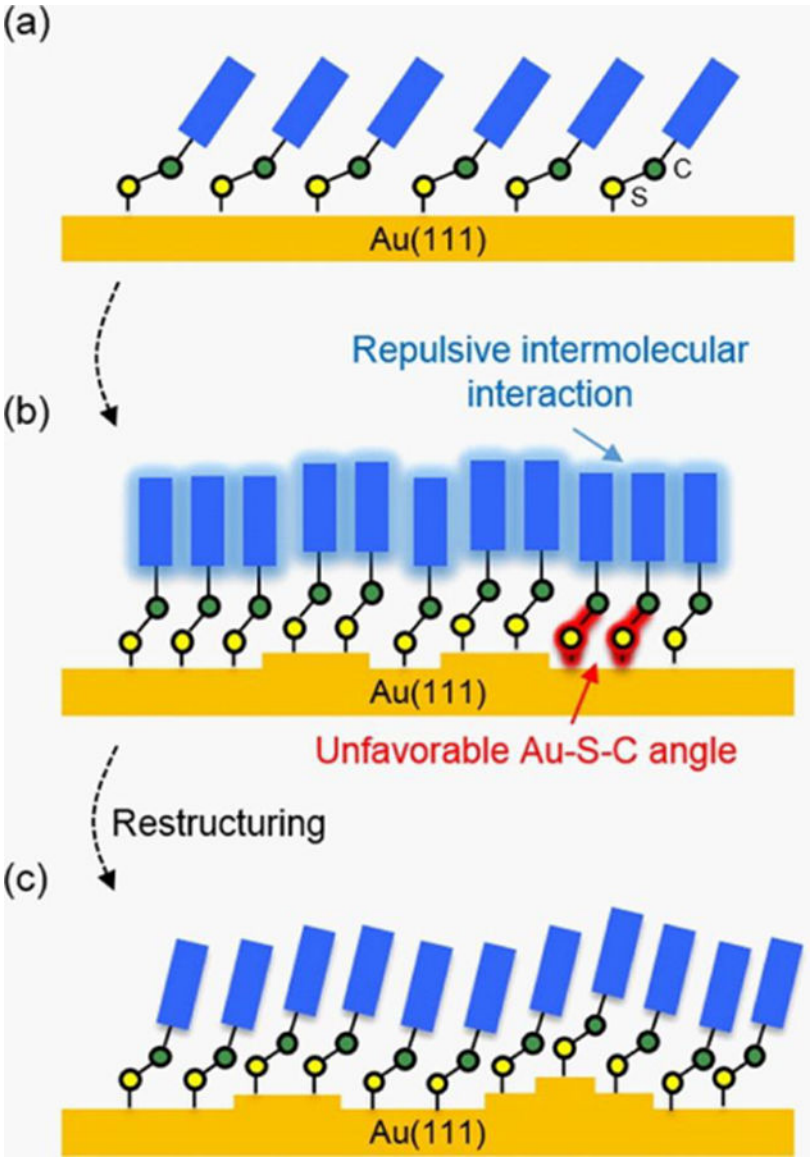

Figure 5.

Structural rearrangement of (a) low coverage, (b) initial high coverage, and (c) equilibrium coverages of aromatic ring-contained molecules on gold. Reprinted with permission from ref 136. Copyright 2016 American Chemical Society.

Table 1.

Summary of Nanoparticle Stability Definitions

Nanoparticle Stability	Definition	Quantitative Characterization		References
		Non-Plasmonic	Plasmonic	
Aggregation	Preservation of primary nanoparticles upon collisions	DLS	LSPR, SERS	17, 28, 31, 45, 64
Metal/Metal Oxide Composition	Unchanged chemical identity and crystallinity of the core during the course of an experiment or relevant time period	EDX, XRD		17, 28, 31, 45, 65, 66, 67
Shape	Preservation of local structure and radius of curvature at the atomic and nanoscales	AFM, HR-TEM, SEM, XRD		17, 28, 31, 43, 45, 46, 68, 69, 70
Size	Preservation of nanoparticle dimension during the course of storage and/or experiment	AFM, DLS, SEM, SAXS, TEM		17, 28, 31, 33, 45, 71, 72, 73, 74
Surface Chemistry	Original surface potential, chemical identity, structure, and functionality of surface chemistry	Low energy ion scattering, XPS, ζ potential		17, 28, 31, 45, 75, 76